Bull. Mater. Sci. (2021)44:129
https://doi.org/10.1007/s12034-021-02419-0

Green synthesis of zinc oxide and copper oxide nanoparticles using *Achillea Nobilis* extract and evaluating their antioxidant and antibacterial properties

SAMANEH MOHAMMAD EBRAHIMZADEH SEPASGOZAR[1], SHARAREH MOHSENI[1,*], BABAK FEIZYZADEH[1] and ALI MORSALI[2]

[1]Department of Chemistry, Quchan Branch, Islamic Azad University, Quchan, Iran
[2]Department of Chemistry, Mashhad Branch, Islamic Azad University, Mashhad, Iran
*Author for correspondence (sh_mohseni2003@yahoo.com)

MS received 13 November 2020; accepted 29 January 2021

Abstract. Recently nanotechnology, as an important area of scientific research, has a considerable growth in numerous fields. Biosynthesis of nanoparticles by using plants and microorganisms has received significant attention due to the growing need to develop environmental technologies in nanoparticle synthesis. The green synthesis of nanoparticles is safe for humans and the environment due to lack of pollution. Plants can act as both stabilizing and reducing agents for the synthesis of metal oxide nanoparticles (MO NPs). The research aim is an illustration of a novel method for the synthesis of zinc oxide nanoparticles (ZnO NPs) and copper oxide nanoparticles (CuO NPs) using *Achillea Nobilis* extract. The crystalline structure and morphology of nanoparticles were studied using characterization techniques such as Fourier transform infrared analysis, ultraviolet–visible spectroscopy studies, X-ray diffraction, field emission scanning electron microscope, and transmission electron microscope methods. The antioxidant activities of ZnO NPs and CuO NPs were evaluated using DPPH assays. Antibacterial activities of nanoparticles were tested against Gram-negative and Gram-positive bacteria using the microdilution method. The results of this study showed that there was a significant relationship between MO NPs resistance and against bacteria.

Keywords. Biosynthesis; zinc oxide nanoparticle; copper oxide nanoparticle; antioxidant activity; antimicrobial activity.

1. Introduction

One of the important research areas in new science is nanotechnology. The size and morphology of nanoparticles lead to the improvement of their specific characteristics. Nanoparticles have distinct properties compared to the bulk form of the same material, thus offering new development in the fields of biomedicine and bio-nanotechnology [1]. Nanoparticles have important applications in the field of natural sciences, such as chemistry, medicine, biology and food processing [2]. The optical, electronic, magnetic and chemical properties of metal oxide nanoparticles (MO NPs) are an important reason for increasing attention. Several methods have been presented for the synthesis of nanoparticles, such as the co-precipitation technique, sol–gel method, thermal decomposition methods and electrochemical methods [3]. In these methods, hazardous solvents and expensive reagents are used for the synthesis of nanoparticles. To address this problem, the present study intends to use eco-friendly reagents and green synthesis. Different studies show that plants seem to be the best candidate because of the faster rate of synthesis, less dangerous procedure and cost-effectiveness [4]. Plants contain biological constituents with antioxidant activities, which have been illustrated to be non-toxic to the environment [5]. The synthesis of nanoparticles with biological resources has opened a modern route for developing an alternative methodology [6]. Recently green synthesis of several nanoparticles from various plants, such as green tea, *Camellia Sinensis*, *Mangiferaindica*, *Azadirachta*, *Indica Clitoria ternatea*, *Solanum nigrum* and *Ocimum Basilicum*, has been reported [2]. Among metal nanoparticles, copper oxide nanoparticles (CuO NPs) have concerned consideration due to their special biological and mechanical properties [7]. CuO is employed in different applications such as catalysis, energy conversion, gas sensor, electronic devices and field emission. CuO NPs are used as an antifungal and antimicrobial agent [8]. Various nanostructures of CuO are synthesized in the form of nanoparticles, nanowire, nanorod, nanoflower and nanoneedle. Several methods have been introduced to produce CuO NPs with different sizes and shapes, such as sonochemical, thermal oxidation, precipitation and

Published online: 06 May 2021

combustion. One of the cheap and cost-effective ways is the precipitation method. It is important because of low energy consumption and good yield [9]. ZnO due to its multi-functional morphological and photonics properties is one of the significant semi-conducting metal oxides [10]. In recent years, zinc oxide nanoparticles (ZnO NPs) have many applications. However, the synthesis of ZnO NPs remains a challenge. Several methods for the synthesis of ZnO NPs have been offered, such as thermal decomposition, sol–gel techniques and precipitation method [11]. Zinc oxide has attracted much interest through its physical and chemical properties such as high stability, wide radiation absorption, catalytic activity, electrochemical coupling coefficient and non-toxic nature. Recently, ZnO NPs were used in many fields such as the rubber industry, pharmaceutical, textile and electronics industries [12]. There are several compounds with antibacterial activity like CuO NPs and ZnO NPs. The antimicrobial properties of metal nanoparticles are attributed to their small size and related high surface area to volume ratio. The protein structure of bacteria changes when direct interaction between nanoparticles and bacterial cells leads to cell membrane permeability [13]. Biomolecules available in plant extracts such as polyphenols, alkaloids, polysaccharides, terpenoids, ascorbic acid and flavonoids have been proposed to a role in nanoparticle formation [14]. The *Achillea Genus* has 19 herbaceous aromatic species in Iran. One of the native species of this genus is *Achillea Nobilis*. Several parts of *Achillea* species are used in traditional medicine because of antiseptic, anti-inflammatory, antihistamine, antioxidant, anti-bleeding, anti-allergic, and cytotoxic activities antitumour, anti-inflammatory, antidiabetic activity [15–17]. *Achillea* species are used in medicine for diuretic, healing wounds, diaphoretic, and are used to reduce sweating and to stop bleeding, amarum and carminativum [18,19]. Various properties of herbal extracts from different species of *Achillea* with antidiabetic, antibacterial, wound healing and gastroprotective activities were attributed to the antioxidant capacity. *Achillea* species with approved antioxidant properties might be considered as a good remedy for the relief of diabetes complications [16]. *A. Nobilis* has biomolecules for reducing and stabilizing nanoparticles. In this study, we adopted a green chemistry approach for the synthesis of CuO NPs and ZnO NPs using the extract plant of the *A. Nobilis* as a reducing agent. For the first time, the extract of this plant was used in the synthesis of MO NPs. This method is simple, green, eco-friendly, economical, and can synthesize MO NPs in a normal atmosphere without any specific physical environment. Furthermore, the antibacterial properties of chemical synthesis of ZnO NPs (Chem-ZnO NPs), green synthesis of ZnO NPs (Bio-ZnO NPs), chemical synthesis of CuO NPs (Chem-CuO NPs), green synthesis of CuO NPs (Bio-CuO NPs) were studied against Gram-negative and Gram-positive bacteria. The antioxidant activity of the synthesized nanoparticles has also been measured based on the free radical scavenging activity by the DPPH (1,1-diphenyl 2-picrylhydrazyl) method.

2. Material and methods

A. Nobilis was collected from Quchan and was identified by the Research Center of Natural for plant sciences, Ferdowsi University of Mashhad (Iran), under identification number 38311 (FUMH). High-purity chemical reagents were purchased from Merck. Copper (II) sulphate pentahydrate ($CuSO_4{\cdot}5H_2O$), zinc nitrate hexahydrate ($ZnNO_3{\cdot}6H_2O$), sodium hydroxide (NaOH), $CuCl_2{\cdot}2H_2O$, zinc sulphate heptahydrate ($ZnSO_4{\cdot}7H_2O$) and deionized water were used in all experimental work.

2.1 *Instruments*

Ultraviolet–visible (UV–vis) spectral analysis was performed on the Cary-8454 spectrophotometer. The morphology of the prepared MO NPs was observed by FE-SEM (S-4160, Hitachi), Zeta potential (CAD, Zeta Compact, France), particle size analyzer (Nano-Sizer, Vasco3, Cordouan, France), EDX (MIRA III, Tescan) and transmission electron microscope (TEM; CM30, Philips) analysis. MO NPs structure and composition were analysed by X-ray diffraction (XRD; PW1730, Philips). Further characterization was done using Fourier transform infrared analysis (FTIR; Spectrum100, Perkin Elmer).

2.2 *Preparation of aqueous A. Nobilis extract*

We used the flowering branch extract of *A. Nobilis*. A quantity of 5 g powder of the plant with 100 ml of deionized water under vigorous mechanical stirring (1000 rpm) was boiled for 20 min at 60°C. Then the extract was cooled at room temperature, filtered through Whatman No. 1 filter paper, and stored at 4°C for further experimental analysis [20] (figure 1).

2.3 *Preparation of nanoparticles via chemical co-precipitation method*

2.3a *Synthesis of CuO NPs:* CuO NPs were synthesized by precipitation method using copper (II) sulphate pentahydrate ($CuSO_4{\cdot}5H_2O$). First, the precursor was

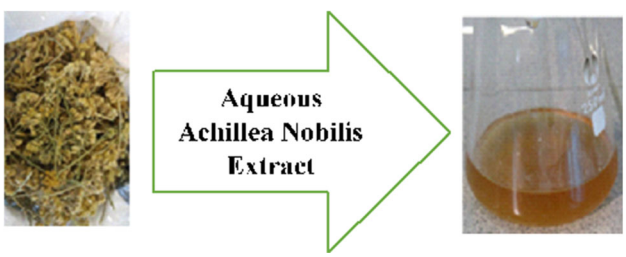

Figure 1. Preparation of aqueous *A. Nobilis* extract.

Figure 2. Preparation of CuO NPs.

Figure 3. Preparation of ZnO NPs.

dissolved in 100 ml deionized water to form a 0.1 M concentration. NaOH solution was slowly added under vigorous stirring until pH reached 8. The brown-black colour precipitate was washed several times using distilled water. Precipitates were dried at 80°C for 16 h. Finally, the precursors were calcined at 400°C for 1 h [21,22] (figure 2).

2.3b *Synthesis of ZnO NPs:* The aqueous solution was prepared by mixing zinc nitrate hexahydrate and sodium hydroxide aqueous solutions. In a typical procedure, 2.283 g of zinc nitrate hexahydrate was dissolved in 75 ml of deionized water, and then 0.67 g of NaOH in 150 ml of deionized water was added dropwise under magnetic stirring. After the addition was completed, the stirring was continued for 30 min and then cooled. The light white colour precipitates (figure 3) were filtered and washed by pure water several times. Then the obtained precipitates were dried at 60°C for 24 h and calcined at 200°C for 2 h [11,23].

2.3c *Biosynthesis of CuO NPs:* CuO NPs were synthesized by dissolving 1.5 g $CuCl_2{\cdot}2H_2O$ in 20 ml of deionized water in a 250 ml Erlenmeyer flask. Then, 100 ml of the aqueous *A. Nobilis* extract was added to the mixture with continuous stirring. The colour of the *A. Nobilis* extract changed to dark green colour, pH of the mixture adjusted by adding sodium hydroxide (1 M) and brown-dark colour precipitate was formed, then filtered and washed with deionized water several times. Later, heated at 80°C for 45 min with ethanol absolute to remove impurities with mild stirring using magnetic stirrer under atmospheric pressure. The mixture was allowed to cool down to room temperature. Black precipitates were obtained and repeatedly washed by deionized water several times [24] (figure 4).

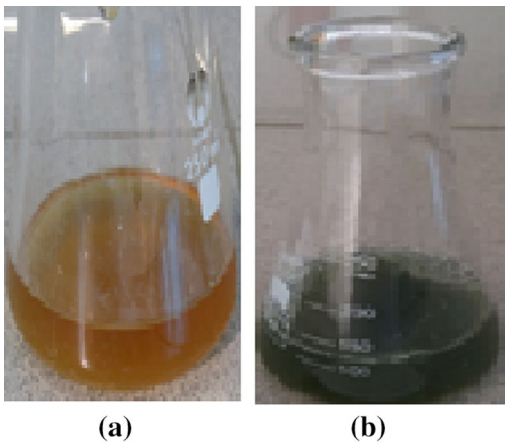

Figure 4. (**a**) Plant extract and (**b**) Bio CuO NPs.

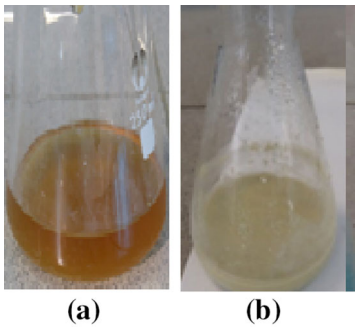

Figure 5. (**a**) Plant extract and (**b**) Bio ZnO NPs.

2.3d *Biosynthesis of ZnO NPs:* ZnO NPs were synthesized by dissolving 5.75 g $ZnSO_4{\cdot}7H_2O$ in 50 ml of deionized water in a 250 ml Erlenmeyer flask. Then, 25 ml of the aqueous *A. Nobilis* extract was added to the mixture, immediately the yellow colour of the *A. Nobilis* extract of the mixture changed to off white colour and heated at 80°C for 2 h with mild stirring using magnetic stirrer under atmospheric pressure. Then 10 ml aqueous solution of sodium hydroxide (25 wt%) was added to the mixtures, and the stirring was continued for 24 h. Creamy precipitates were obtained and repeatedly washed by deionized water several times till pH reached 7. The washed precipitates were dried at 140°C for 8 h. Finally, the precursors were calcined at 500°C for 1 h [25] (figure 5).

2.4 *Antioxidant activity (DPPH free radical scavenging assay)*

The antioxidant activity of MO NPs was examined based on the scavenging effect on the stable DPPH free radical activity. The ethanolic solution of DPPH (0.1 mM) (3 ml) was added to 600 µl of MO NPs solution with different concentrations (1000, 500, 100 and 20 ppm). DPPH solution

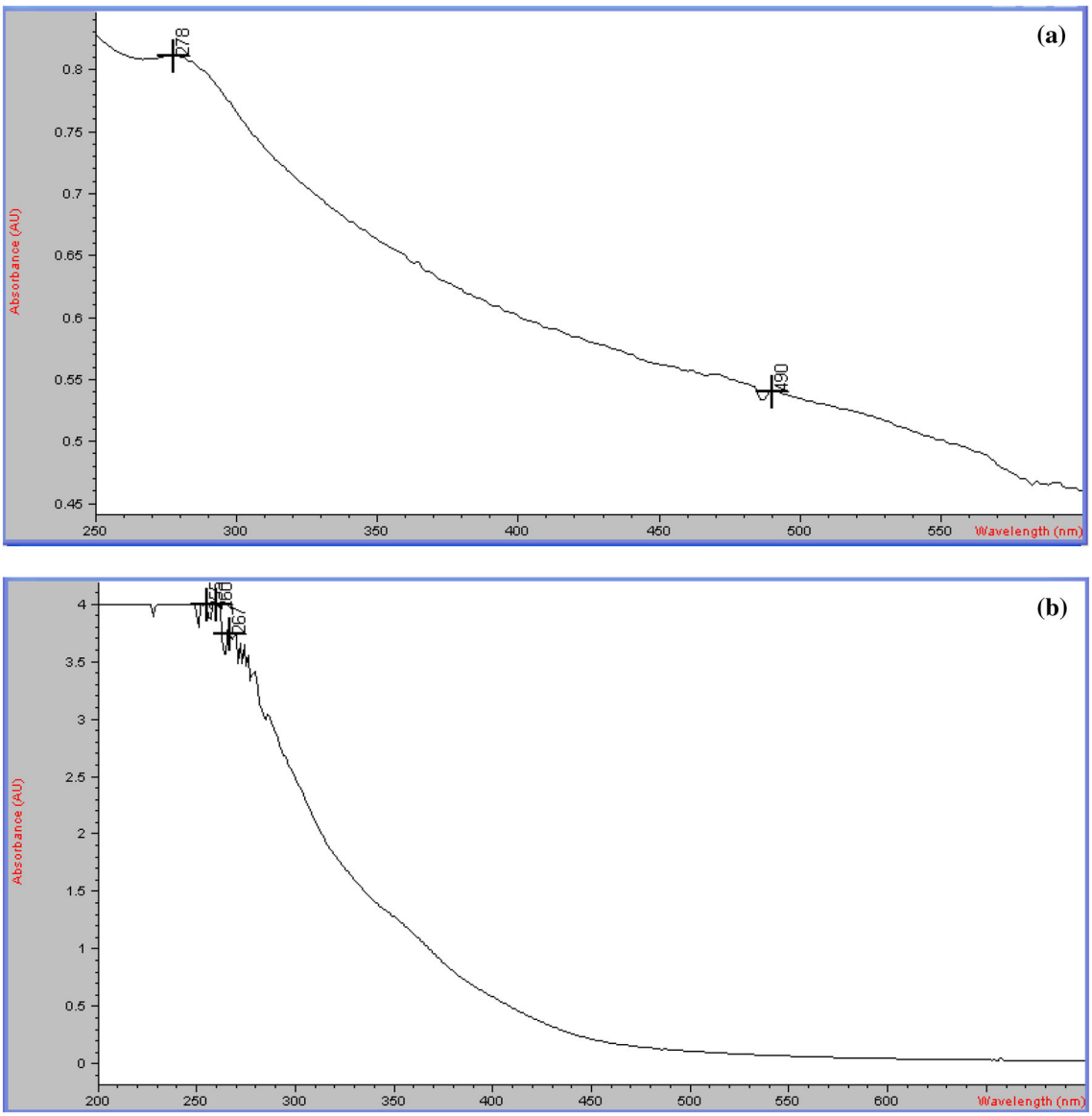

Figure 6. UV–vis absorption spectra of CuO NPs using (**a**) chemical co-precipitation method and (**b**) green method.

was freshly prepared and kept in the dark at 4°C. Ethanol 96% was added, and the mixture was shaken vigorously. The mixture was left to stand for 30 min, and absorbance was measured at 517 nm. Ethanol was used to set the absorbance zero. A blank sample containing the same amount of ethanol and DPPH was also prepared. The reducing power of the extracts increased in a concentration-dependent manner. The DPPH free radical scavenging activity was determined from the different bio-metal oxide NPs at different concentrations (1000, 500, 100 and 20 ppm). This assay showed that an increase in the concentration of MO NPs led to a rise in the radical scavenging activity [26]. According to the following equation, the radical scavenging activities of the samples were calculated and expressed as a percentage of inhibition.

$$\text{Percent } (\%) \text{ inhibition of DPPH activity} = [(\text{AB} - \text{AA})/\text{AB}] \times 100 \quad (1)$$

In equation (1), AA and AB are the absorbance values of the test and the blank samples. A percent inhibition *vs.* concentration curve was plotted, and the concentration of the sample required for 50% inhibition was specified [27].

2.5 *Antibacterial assay*

To evaluate the antibacterial effects, inhibition zone diameter for two multidrug-resistant pathogenesis, *Escherichia coli* PTTC 1399 (Gram-negative bacteria) and *Staphylococcus aureus* 1112 PTTC (Gram-positive bacteria) bacteria using

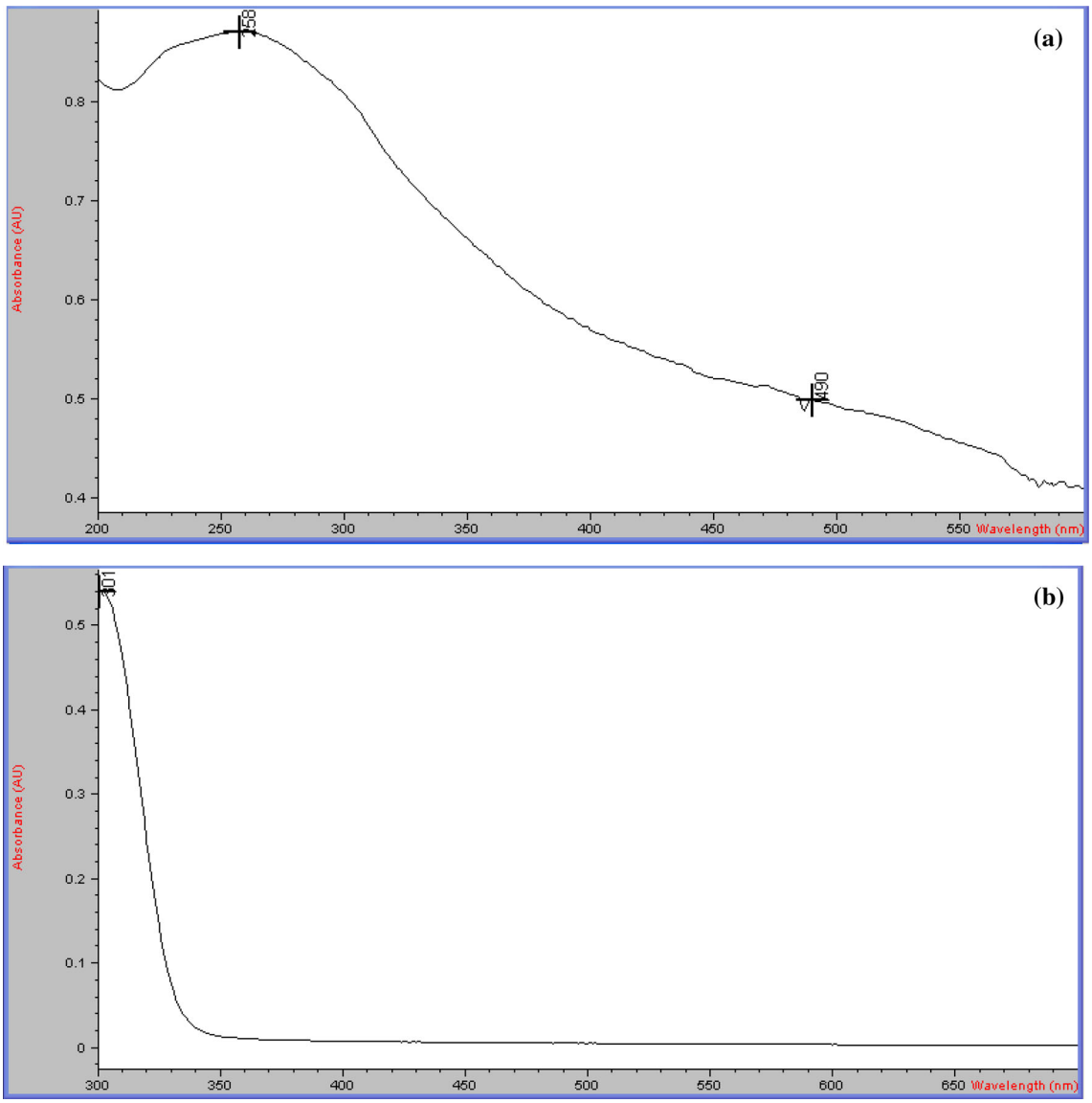

Figure 7. UV–vis absorption spectra of ZnO NPs using (**a**) chemical co-precipitation method and (**b**) green method.

agar well diffusion method, was measured. Antibacterial activities of CuO and ZnO NPs using the chemical co-precipitation method and green method were investigated [28]. First, for the bacterial strain, the cell suspension with 0.5 *McFarland* turbidity (1.5×10^8 CFU ml^{-1}) was prepared, and each well of the ELISA plate was filled with 200 µl of Muller-Hinton broth (MHB), and then 100 µl of MO NPs was poured in the first cast well. Afterwards, 100 µl of this mixture was removed and transferred to the next well. This process continued to the last well. Finally, the concentrations of MO NPs (200, 100, 75, 50 and 25 µg ml^{-1}) were obtained [29].

2.6 *Statistical analysis*

Data of all analyses were displayed as the mean ± standard deviation. Statistical analysis was conducted with the analysis of variance (ANOVA) procedure using SPSS Version 20 software. The differences among the experimental data were determined using the least significant difference method. A value of $P < 0.05$ was considered statistically significant.

3. Results

3.1 *UV-spectrophotometer analysis*

The synthesized nanoparticles via chemical co-precipitation and green method were characterized through UV–vis absorption. A quantity of 4 ml of the dilute colloid solution was added into a quartz cuvette, and the results are shown in figures 6 and 7.

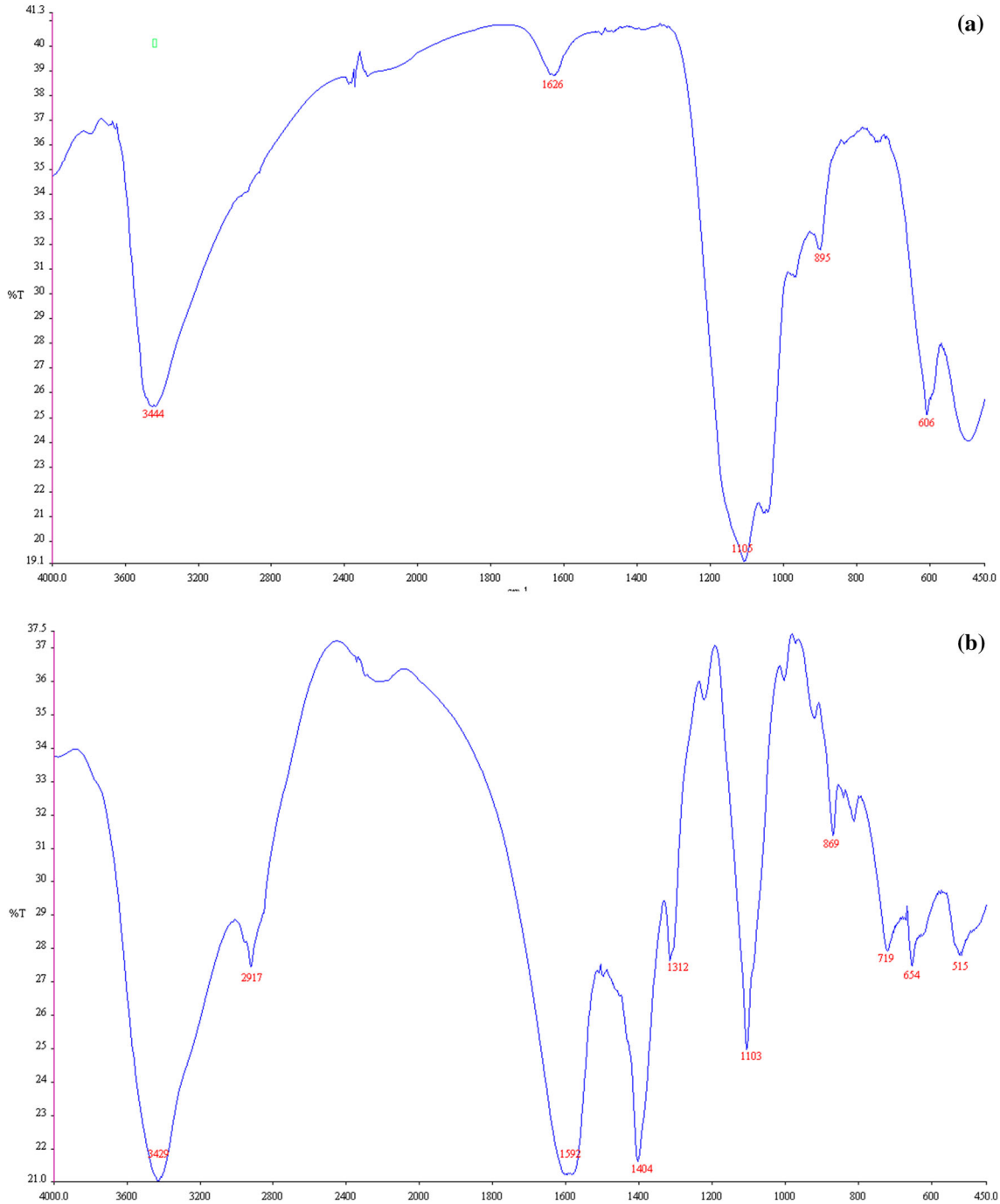

Figure 8. FT-IR spectra of CuO NPs using (**a**) chemical co-precipitation method and (**b**) green method.

3.2 *FT-IR analysis*

Fourier transform infrared spectroscopy (FT-IR) can be used to characterize the physical properties of nanomaterials and their functions [14]. FTIR spectrum of the extract showed a band between 2890 and 3400 cm^{-1}. Purified samples of CuO NPs and ZnO NPs were dried and mixed well with 1% KBr plate of the powder samples for pellet preparation for FT-IR measurements. FT-IR analysis was carried for the reduction of copper and zinc ions with a spectral range of 400–4000 cm^{-1}. Figure 8 and table 1 show bands at 3429, 1592, 1103, 869 and 654 cm^{-1} for the CuO NPs using the chemical co-precipitation method, and FT-IR spectra for the green method showed bands at 3444, 1626, 1105, 895 and 606 cm^{-1} [30]. FT-IR spectra of ZnO NPs illustrated peaks in the range of 450–4000 cm^{-1} (figure 9a and b, and table 2).

Table 1. Possible assignments and peak area values of FT-IR spectra for Chem-CuO NPs and biosynthesized using *A. Nobilis* extract.

Frequency (cm^{-1})		
Chem-CuO NPs	Bio-CuO NPs	Possible assignment
3429	3444	Amide N–H stretching
1592	1626	C=C stretching (alkene)
1103	1105	O–H bending (alcohols)
654	606	Stretching vibration of Cu–O

3.3 *TEM and FESEM analysis*

TEM analysis is the most common method to determine the size, shape and distribution of the nanoparticles. For the preparation of the TEM, a small amount of powder was dispersed in high-purity ethanol via ultrasonic equipment. Figure 10a and b shows high-resolution images of CuO NPs. The surface morphology of synthesized ZnO NPs prepared from *A. Nobilis* aqueous extract was characterized by field emission scanning electron microscopic (FESEM) analysis. The biosynthesized ZnO NPs were observed using FESEM, and the resultant images at different magnification levels and EDX spectrum are shown in figures 11 and 12.

3.4 *X-ray diffraction*

For further investigations, XRD are addressed as a versatile, non-destructive analytical method. In general, XRD is used for the identification and quantitative determination of various crystalline forms, known as 'phases' of the compound, which presents in powder and solid samples [31]. The crystalline structure of MO NPs (a bit of powdered sample of CuO NPs and ZnO NPs from 0.4 M $CuCl_2{\cdot}2H_2O$ and 0.4 M $ZnSO_4{\cdot}7H_2O$) was determined by XRD analysis using an X-Ray Diffraction Unit (PW1730, Philips) at room temperature. The XRD pattern of bio-synthesized CuO and ZnO NPs from aqueous extract of *A. Nobilis* is shown in figure 13a and b. The XRD of the synthesized CuO nanoparticles shows broad peaks at 2θ values of 35.46, 38.66, 48.77, 61.50, 66.35, 72.51 and 75.07 were assigned to (002), (111), ($\bar{2}02$), ($\bar{1}13$), ($\bar{3}13$), (221) and ($\bar{2}22$) planes, respectively. All the diffraction peaks can be understood as a monoclinic structure of CuO, which is comparable with ICCD Ref. No. 04-012-7238. The XRD of the synthesized ZnO NPs shows broad peaks at 2θ values of 31.86, 34.50, 36.35, 47.57, 47.67, 56.64, 56.88, 62.94, 63.09, 66.49, 66.73, 68.05, 69.20, 69.38, 72.64 and 77.16 assigned to (100), (002), (101), (102), (102), (110), (103), (103), (200), (200), (112), (201), (201), (004) and (202) planes, respectively. All the diffraction peaks were well indexed to the hexagonal phase of ZnO, which are comparable with ICCD Ref. No. 04-015-4060.

3.5 *Zeta potential particle size analysis*

The particle size and zeta potential of green synthesized CuO NPs, and ZnO NPs were determined in an aqueous solution using a particle size analyzer (Nano-Sizer, Vasco3, Cordouan, France). The average particle size and polydispersity index (PDI) of green synthesized CuO NPs and ZnO NPs are presented in figure 14a and b. PDI is a parameter used to define the homogeneity of the nanoparticles [32]. In the present study, for the obtained CuO NPs the negative zeta potential was found at –19.74 mV at pH = 6.72 and 24.28°C. The size distribution and zeta potential of the prepared nanoparticles were measured at pH = 6.64 and 24.11°C. For the obtained ZnO NPs, the zeta potential value was also measured, affording to –23.33 mV. It is well known that the surface charge and size distribution play key roles in the biological activity of prepared NPs.

3.6 *Antioxidant and antibacterial activities*

The results confirmed that the nanoparticles have antioxidant activity. Figure 15 demonstrates a significant reduction in the concentration of DPPH that is due to the scavenging ability of methanolic extract of all the nanoparticles. Evaluation of the antioxidant activity is obtained on the basis of the free radical trapping [33]. The presence of metal ions in extracts, as a natural component of plants, is often ignored. Metal chelation by polyphenolic compounds is widely considered as another mechanism of their antioxidant activity [34]. The studies show that in the absence of flavonoids, metallic ions could not promote inhibition of DPPH radical. Therefore, the observed changes could be attributed to the formation of flavonoid–metal complexes. Researches show that different metal content could be extracted from plants [35]. There are different quantities of Zn in wild-growing herbaceous plants like *A. Nobilis* [36].

In agar, well diffusion method MO NPs showed significant antibacterial activity on all the two bacterial strains [28]. Studies on different species have shown that the plant extract has good antibacterial properties. Chaplygin *et al* [36] investigated the antibacterial properties of *A. Nobilis*. The comparison of our studies with Chaplygin data shows that the minimum inhibitory concentration (MIC) of bio-CuO NPs was lower than *A. Nobilis* extract, while in Chem-ZnO NPs, Chem-CuO NPs and bio-ZnO inhibitory concentrations were higher than the extract [37]. Results of the bactericidal effect of the metal oxide NPs on the pathogen bacteria are shown in tables 3 and 4. Of the bacterial strains tested, Chem-ZnO NPs showed a low inhibitory effect on the growth of Gram-negative bacteria (*E. coli*, 5.95 mm), at a concentration of 25 μg ml^{-1}. The Bio-CuO NPs strongly inhibited the growth of Gram-positive bacteria (*S. aureus*, 12.2 mm) at a concentration of 200 μg ml^{-1} [1,38]. The MIC and the minimum bactericidal concentration (MBC) of

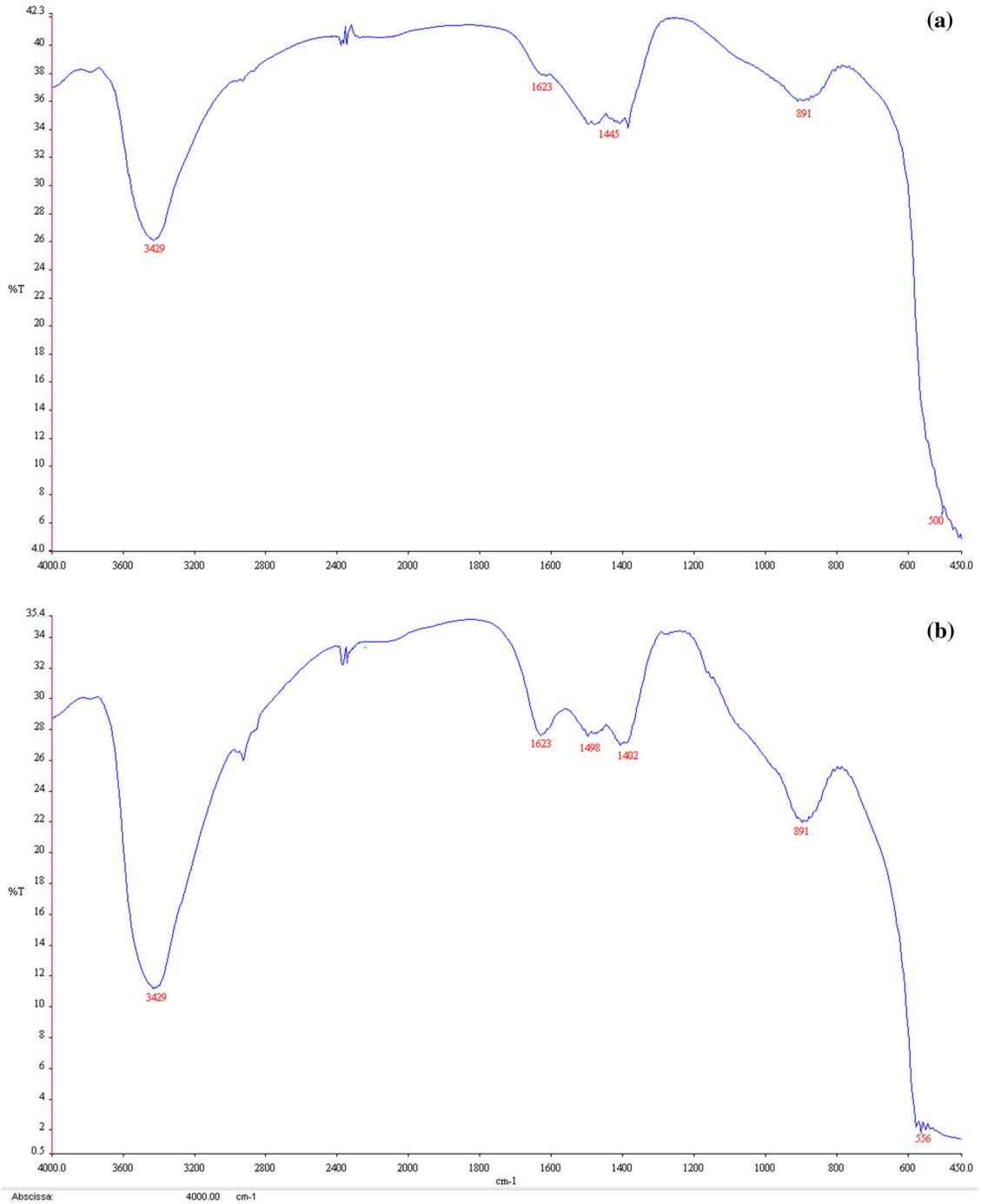

Figure 9. FT-IR spectra of ZnO NPs using (**a**) chemical co-precipitation method and (**b**) green method.

MO NPs for the antibacterial activities are presented in table 5.

4. Discussions

In the present investigation, the green synthesis method is used to synthesize the CuO NPs and ZnO NPs using *A. Nobilis* aqueous extract, which is cost-effective and is an eco-friendly approach compared to other methods. The challenge of this method was to maintain the calcination temperature at 500°C, which resulted in forming 14–56 nm sizes of ZnO NPs. This practice was in line with the previous investigations such as Matinise *et al* [39], Mornani *et al* [40] and Thema *et al* [41]. The characteristics of the synthesized CuO NPs and ZnO NPs were studied using UV–vis spectrophotometer, FT-IR, TEM, SEM with EDX, and XRD analyses. The UV–vis spectra analysis revealed a

Table 2. Possible assignments and peak area values of FT-IR spectra for Chem-ZnO NPs and biosynthesized using *A. Nobilis* extract.

Frequency (cm^{-1})		
Chem-ZnO NPs	Bio-ZnO NPs	Possible assignment
3429	3429	O–H stretching vibrations
1623	1623	C=C stretching (alkene)
1445	1498	Aromatic –CH stretching vibrations
532	556	Stretching vibration of Zn–O

strong absorbance between 250 and 300 nm, suggesting the formation of CuO NPs [7]. From this analysis, the absorbance peak was found at 301 nm for ZnO NPs, which is an acceptable value for these nanoparticles [42]. FT-IR spectroscopic measurements were carried out to identify the possible biomolecules in extracts for the efficient stabilization of MO NPs [14]. In this research extract, FT-IR showed stretching vibrations of the primary and secondary amines, O−H stretching of alcohols and C−H stretching of alkanes. FT-IR analysis of this study was similar to those of previous studies, in which CuO NPs and ZnO NPs were green synthesized [30]. The broad peak obtained for ZnO

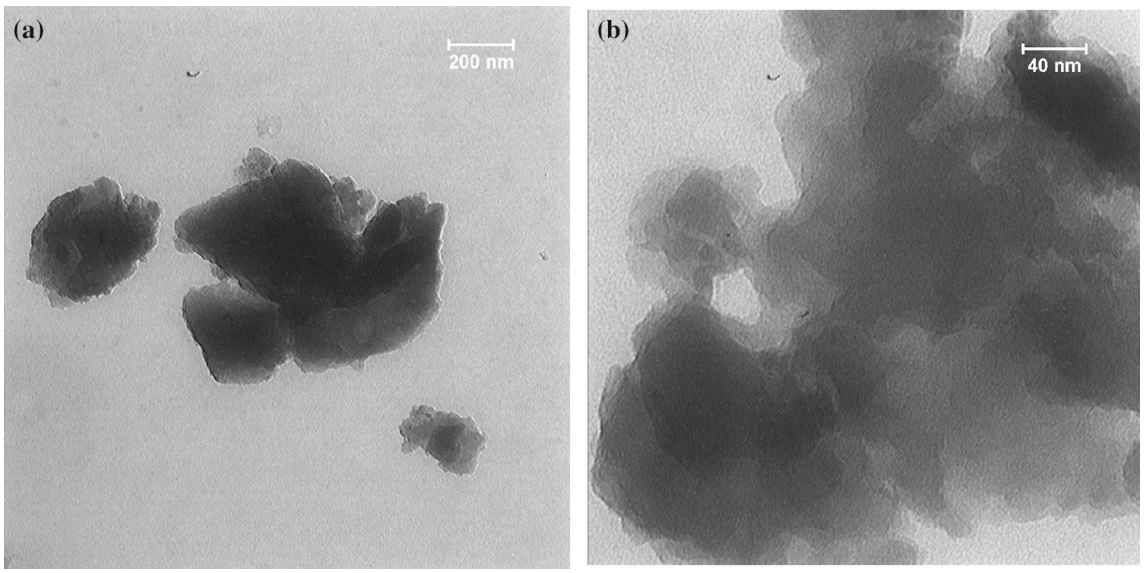

Figure 10. (**a**, **b**) TEM images of synthesized CuO NPs.

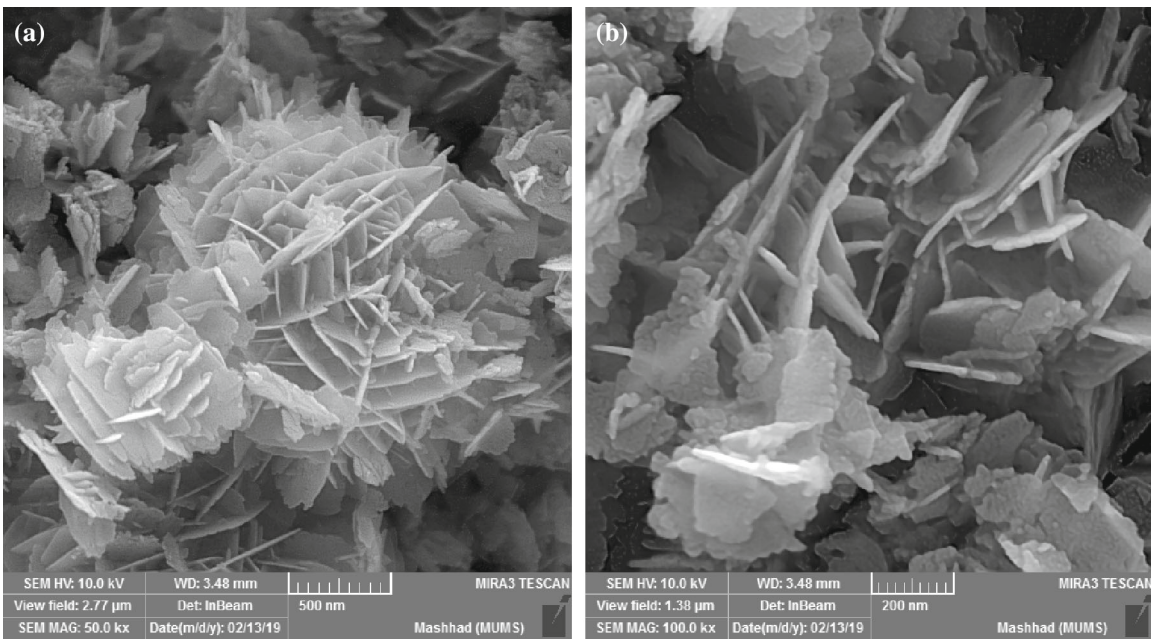

Figure 11. Microscopic images of green synthesized MO NPs: FESEM images of ZnO NPs (**a**, **b**) calcined at 500°C.

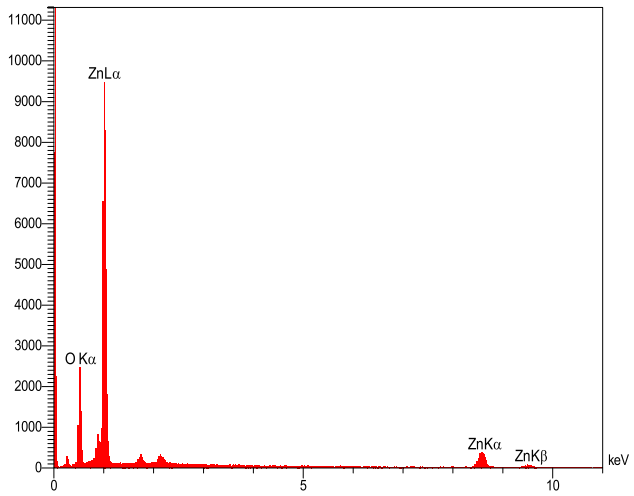

Figure 12. EDX spectrum of ZnO NPs.

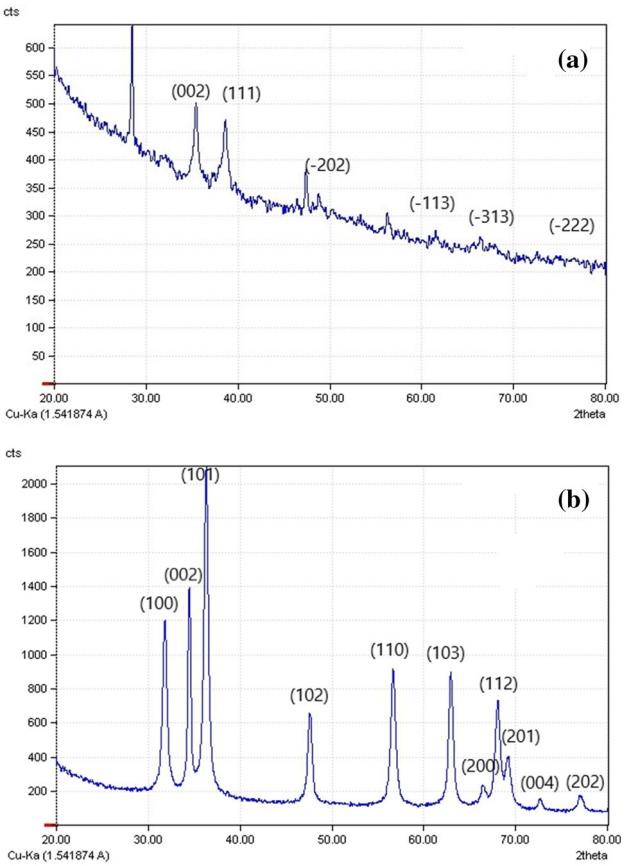

Figure 13. XRD patterns of (**a**) CuO NPs and (**b**) ZnO NPs.

NPs at 3429 corresponded to OH stretching vibrations and peak in the range of 1623 corresponded to C=C stretching (alkene). The other peaks obtained at 1445 and 1498 demonstrated the presence of aromatic –CH stretching vibrations. The stretching bands at 556 and 532 cm^{-1} are

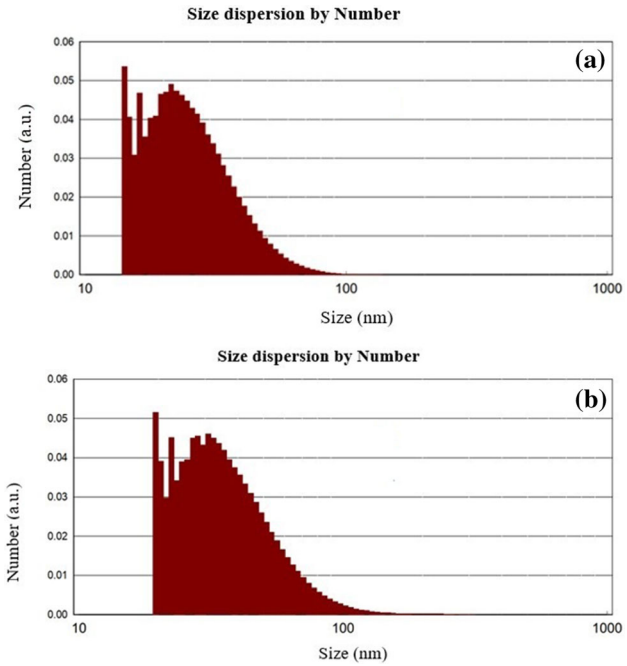

Figure 14. Particle size distribution: (**a**) CuO NPs and (**b**) ZnO NPs.

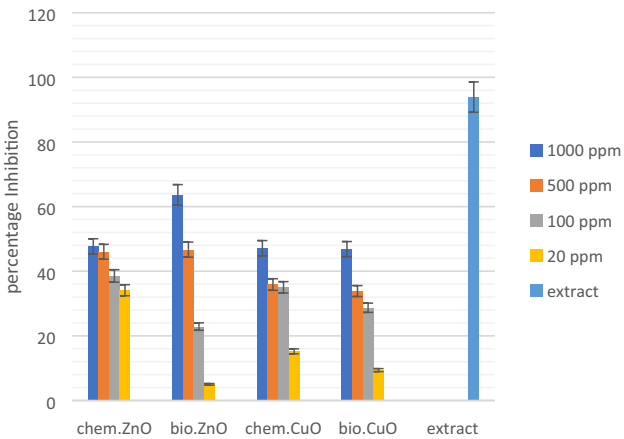

Figure 15. DPPH radical scavenging activity of nanoparticles and extract *A. Nobilis.*

related to Zn–O absorption, and at 600 and 668 cm^{-1} are related to Cu–O absorption further indicating ZnO and CuO NPs formation [8,43].

The TEM study of CuO NPs is carried out to understand the crystalline characteristics of the nanoparticles. These particles are observed to be monoclinic, and the size is found to be in the range of 15–25 nm [44].

The biosynthesized ZnO NPs were observed using FESEM. The nanoparticles possess highly uniform hexagonal particles. Noticeably, most of the nanoparticles are uniform in size. The NPs are a little agglomerated, and the size of ZnO NPs has increased slightly after annealing [30].

Table 3. Zone of inhibition (mm in dia.) for Chem-ZnO NPs and Chem-CuO NPs on the pathogen bacteria.

Microorganism	Concentration	Chem-CuO NPs	Chem-ZnO NPs	Ampicillin	Gentamicin
Staphylococcus aureus	25	7.5 ± 0.31	6.85 ± 0.36	18 ± 0.85	17 ± 0.31
	50	7.8 ± 0.22	7.6 ± 0.21		
	75	8.1 ± 0.32	8.4 ± 0.27		
	100	8.8 ± 0.25	8.8 ± 0.32		
	200	9.2 ± 0.18	10.4 ± 0.40		
Escherichia coli	25	6.7 ± 0.23	5.95 ± 0.24	13 ± 0.22	16 ± 0.55
	50	8.3 ± 0.14	6.52 ± 0.25		
	75	8.9 ± 0.18	7.38 ± 0.54		
	100	9.23 ± 0.25	7.82 ± 0.17		
	200	9.51 ± 0.32	8.11 ± 0.15		

Table 4. Zone of inhibition (mm in dia.) for Bio-ZnO NPs and Bio-CuO NPs on the pathogen bacteria.

Microorganism	Concentration	Bio-CuO NPs	Bio-ZnO NPs	Ampicillin	Gentamicin
Staphylococcus aureus	25	8.2 ± 0.15	7.30 ± 0.38	18 ± 0.85	17 ± 0.31
	50	9.3 ± 0.28	8 ± 0.24		
	75	10.5 ± 0.35	9.2 ± 0.35		
	100	11.25 ± 0.38	10.52 ± 0.25		
	200	12.20 ± 0.14	11.42 ± 0.30		
Escherichia coli	25	7.3 ± 0.34	6.55 ± 0.25	13 ± 0.23	16 ± 0.55
	50	8.2 ± 0.14	7.34 ± 0.37		
	75	8.0 ± 0.21	8.15 ± 0.41		
	100	9.35 ± 0.15	8.85 ± 0.22		
	200	9.7 ± 0.25	9.27 ± 0.27		

Table 5. MIC and MBC (μg ml^{-1}) for metal oxide nanoparticles against selected pathogens.

	MICs/MBCs			
Microorganism	Chem-CuO NPs	Bio-CuO NPs	Chem-ZnO NPs	Bio-ZnO NPs
Staphylococcus aureus	6.25/12.5	1.56/6.25	3.12/—	12.5/25
Escherichia coli	12.5/25	6.25/12.5	6.25/—	6.25/50

XRD analysis indicated the crystalline nature of ZnO and CuO NPs synthesized by *A. Nobilis* aqueous extract. These peaks were in good agreement with the reported literature [42]. The diameter of the synthesized MO NPs was calculated using the Debye Scherrer formula by the following equation:

$$D = 0.89\,\lambda/\beta(\cos\theta), \tag{2}$$

where D is the average crystalline size, λ the CuKα radiation wavelength, β the full-width at half-maximum (FWHM) in radians of the CuO (002), ZnO (101) lines, and θ the scattering angle in degree. The average crystallite size D was calculated using equation (2), which was found to be 6.5 and 14.7 nm for CuO and ZnO NPs, respectively.

Zeta potential particle size analysis ensures the high stability of the formed ZnO NPs as well [31]. The average particle size of nanoparticles was obtained using a particle size analyzer. It was observed that the size of CuO NPs was within a range of 5.89–24.55 nm, and the size of ZnO NPs was 14–56 nm.

Antioxidant activity results confirmed that the nanoparticles have antioxidant activity. Methanolic extract of *A. Nobilis* has greater antioxidant activity as compared to MO NPs [27]. Antibacterial results of MIC and MBC of MO NPs up to 200 μg ml^{-1} against the desired bacteria were determined using the dilution method. The lowest MBC value was noticed in Bio-ZnO NPs against *E. coli* (50 μg ml^{-1}). The highest MIC value was noticed in Bio-CuO NPs

against *S. aureus* (1.56 μg ml^{-1}). The highest MBC value was noticed in Bio-CuO NPs against *S. aureus* (6.25 μg ml^{-1}). Also, chem-ZnO NPs were not capable of interfering with bacterial growth but were shown to be inhibitory, which is in line with previous observations reported by Anbukkarasi *et al* [45].

5. Conclusions

In this study, a simple, safe, economical and green process has been developed to synthesize MO NPs. For the first time, we presented an effective method for the synthesis of the CuO and ZnO NPs via *A. Nobilis* extracts without any pollution. The MO NPs were confirmed by UV-spectrophotometer, FT-IR, particle size, EDX, FESEM and TEM analyses. The antioxidant and antimicrobial activities of all nanoparticles are shown. We compared the synthesis of nanoparticles via green and chemical methods for antibacterial and antioxidant properties. Our results indicate that nanoparticles were effective against both the Gram-positive and Gram-negative bacterial strains. The inhibitory effect of the above nanoparticles on Gram-positive *S. aureus* was more than Gram-negative *E. coli*. Bio-CuO NPs, Bio-ZnO NPs and Chem-CuO NPs can also inhibit the growth of bacteria. The results confirmed that the prepared nanoparticles have proper physicochemical properties for pharmaceutical and biomedical applications.

References

[1] Sravanthi M, Muni Kumar D, Usha B, Ravichandra M, Mahendra Rao M and Hemalatha K P J 2016 *Int. J. Adv. Res.* **4** 589

[2] Rajendran S P and Sengodan K 2017 *J. Nanosci.* **2017** 1

[3] Majidi S, Zeinali Sehrig F, Farkhani S M, Soleymani Goloujeh M and Akbarzadeh A 2016 *Artif. Cells Nanomed. Biotechnol.* **44** 722

[4] Basnet P, Chanu T I, Samanta D and Chatterjee S 2018 *J. Photochem. Photobiol. B Biol.* **183** 201

[5] Namvar F, Azizi S, Ahmad M B, Shameli K, Mohamad R, Mahdavi M *et al* 2015 *Res. Chem. Intermed.* **41** 5723

[6] Ebrahimzadeh M A, Naghizadeh A, Amiri O, Shirzadi-Ahodashti M and Mortazavi-Derazkola S 2020 *Bioorg. Chem.* **94** 103425

[7] Sankar R, Manikandan P, Malarvizhi V, Fathima T, Shivashangari K S and Ravikumar V 2014 *Spectrochim. Acta Part A Mol. Biomol. Spectrosc.* **121** 746

[8] Shi L-B, Tang P-F, Zhang W, Zhao Y-P, Zhang L-C and Zhang H 2017 *Trop. J. Pharm. Res.* **16** 185

[9] Phiwdang K, Suphankij S, Mekprasart W and Pecharapa W 2013 *Energy Procedia* **34** 740

[10] Rad S S, Sani A M and Mohseni S 2019 *Microb. Pathog.* **131** 239

[11] Suntako R 2015 *Bull. Mater. Sci.* **38** 1033

[12] Mohan A C and Renjanadevi B 2016 *Procedia Technol.* **24** 761

[13] Shaaban M and El-Mahdy A M 2018 *IET Nanobiotechnol.* **12** 741

[14] Sorbiun M, Shayegan Mehr E, Ramazani A and Mashhadi Malekzadeh A 2018 *Nanochem. Res.* **3** 1

[15] Alsohaili S A, Al-fawwaz A T, Afshari M, Rahimmalek M, Miroliaei M, Azimi R *et al* 2014 *Eur. Sci. J.* **31** e1800075

[16] Afshari M, Rahimmalek M and Miroliaei M 2018 *Chem. Biodivers.* **15** e1800075

[17] Azimi R, Sefidkon F and Monfared A 2016 *Iran J. Med. Aromat. Plants* **31** 954

[18] Ghani A, Azizi M, Hassanzadeh-Khayyat M and Pahlavanpour A A 2008 *J. Essent. Oil Bear. Plants* **11** 460

[19] Motavalizadehkakhky A, Shafaghat A, Zamani H A, Akhlaghi H, Mohammadhosseini M, Mehrzad J *et al* 2013 *J. Med. Plants Res.* **7** 1280

[20] Ahmed S, Chaudhry S A and Ikram S 2017 *J. Photochem. Photobiol. B Biol.* **166** 272

[21] Nagajyothi P C, Muthuraman P, Sreekanth T V M, Kim D H and Shim J 2017 *Arab. J. Chem.* **10** 215

[22] Hwa K Y and Karuppaiah P 2019 *Mater. Sci. Forum* **962** 51

[23] Ramesh M, Anbuvannan M and Viruthagiri G 2015 *Spectrochim. Acta Part A Mol. Biomol. Spectrosc.* **136** 864

[24] Hassan K H, Saadi S K, Jarullah A A and Harris P 2018 *Pakistan J. Sci. Ind. Res. Ser. A Phys. Sci.* **61** 59

[25] Zhu Y and Zhou Y 2008 *Appl. Phys. A* **92** 275

[26] Park C H, Yeo H J, Baskar T B, Park Y E, Park J S, Lee S Y *et al* 2019 *Antioxidants* **8** 75

[27] Majumdar M and Parihar P S 2012 *Asian J. Plant Sci. Res.* **2** 95

[28] Naika H R, Lingaraju K, Manjunath K, Kumar D, Nagaraju G, Suresh D *et al* 2015 *J. Taibah Univ. Sci.* **9** 7

[29] Khatami M, Aflatoonian M R, Azizi H, Mosazade F, Hoshmand A, Nobre M A L *et al* 2017 *Int. J. Basic Sci. Med.* **2** 166

[30] Sorbiun M, Mehr E S, Ramazani A and Fardood S T 2018 *Int. J. Environ. Res.* **12** 29

[31] El-Naggar M E, Hassabo A G, Mohamed A L and Shaheen T I 2017 *J. Colloid Interface Sci.* **498** 413

[32] Kanagasubbulakshmi S and Kadirvelu K 2017 *Def. Life Sci. J.* **2** 422

[33] Ghasemian Dazmiri M, Alinezhad H, Hossaini Z and Bekhradnia A R 2020 *Appl. Organomet. Chem.* **34** 1

[34] Pyrzynska K and Pękal A 2013 *Anal. Methods* **5** 4288

[35] Pekal A, Pyrzynska K, Pękal A and Pyrzynska K 2015 *Int. J. Food Sci. Nutr.* **66** 58

[36] Chaplygin V, Mandzhieva S, Litvinov Y, Kravtsova N, Sherstnev A, Chernikova N *et al* 2020 *Web Conf.* **169** 01003

[37] Vijayakumar S, Vaseeharan B, Malaikozhundan B and Shobiya M 2016 *Biomed. Pharmacother.* **84** 1213

[38] Kalyani R L, Venkatraju J, Kollu P, Rao N H and Pammi S V N 2015 *Korean J. Chem. Eng.* **32** 911

[39] Matinise N, Fuku X G, Kaviyarasu K, Mayedwa N and Maaza M 2017 *Appl. Surf. Sci.* **406** 339
[40] Mornani E G, Mosayebian P, Dorranian D and Behzad K 2016 *J. Ovonic Res.* **12** 75
[41] Thema F T, Manikandan E, Dhlamini M S and Maaza M 2015 *Mater. Lett.* **161** 124
[42] Getie S, Belay A, Chandra Reddy A R and Belay Z 2017 *J. Nanomed. Nanotechnol.* **8** 4
[43] Santhoshkumar J, Kumar S V and Rajeshkumar S 2017 *Resour. Technol.* **3** 459
[44] Srivastava S 2013 *IOSR J. Appl. Phys.* **5** 61
[45] Anbukkarasi V, Srinivasan R and Elangovan N 2015 *Int. J. Pharm. Sci. Rev. Res.* **33** 110